Low-energy neutron-deuteron reactions with N^{3}LO chiral forces

J. Golak, R. Skibiński, K. Topolnicki, and H. Witała

M. Smoluchowski Institute of Physics,

Jagiellonian University, PL-30059 Kraków, Poland

E. Epelbaum and H. Krebs

Institut für Theoretische Physik II, Ruhr-Universität Bochum, D-44780 Bochum, Germany

H. Kamada

Department of Physics, Faculty of Engineering,

Kyushu Institute of Technology, Kitakyushu 804-8550, Japan

Ulf-G. Meißner

Helmholtz-Institut für Strahlen- und Kernphysik and Bethe Center for Theoretical Physics,

Universität Bonn, D–53115 Bonn, Germany

and

Institute for Advanced Simulation, Institut für Kernphysik, Jülich Center for Hadron Physics,

and JARA - High Performance Computing Forschungszentrum Jülich, D-52425 Jülich, Germany

V. Bernard

Institut de Physique Nucléaire, CNRS/Univ. Paris-Sud 11,

(UMR 8608), F-91406 Orsay Cedex, France

P. Maris and J. Vary

Department of Physics and Astronomy,

Iowa State University, Ames, Iowa 50011, USA

S. Binder, A. Calci, J. Langhammer, and R. Roth

Institut für Kernphysik, Technische Universität Darmstadt, 64289 Darmstadt, Germany

K. Hebeler

Institut für Kernphysik,

Technische Universität Darmstadt,

64289 Darmstadt, Germany

arXiv:1410.0756v3 [nucl-th] 7 Oct 2014

and

Extreme Matter Institute EMMI, GSI Helmholtzzentrum für Schwerionenforschung GmbH, 64291 Darmstadt, Germany

A. Nogga

Institut für Kernphysik, Institute for Advanced Simulation and Jülich Center for Hadron Physics, Forschungszentrum Jülich, D-52425 Jülich, Germany

S. Liebig and D. Minossi

Institut für Kernphysik and Jülich Center for Hadron Physics, Forschungszentrum Jülich, D-52425 Jülich, Germany

(Dated: October 8, 2014)

Abstract

We solve three-nucleon Faddeev equations with nucleon-nucleon and three-nucleon forces derived consistently in the framework of chiral perturbation theory at next-to-next-to-next-to-leading order in the chiral expansion. In this first investigation we include only matrix elements of the three-nucleon force for partial waves with the total two-nucleon (three-nucleon) angular momenta up to 3 (5/2). Low-energy neutron-deuteron elastic scattering and deuteron breakup reaction are studied. Emphasis is put on A_y puzzle in elastic scattering and cross sections in symmetric-space-star and neutron-neutron quasi-free-scattering breakup configurations, for which large discrepancies between data and theory have been reported.

PACS numbers: 21.45.+v, 24.70.+s, 25.10.+s, 25.40.Lw

I. INTRODUCTION

A special place among few-body systems is reserved for the three-nucleon (3N) system, for which a mathematically sound theoretical formulation in the form of Faddeev equations exists, both for bound and scattering states. Over the past few decades algorithms have been developed to solve numerically three-nucleon Faddeev equations for any dynamical input which, in addition to nucleon-nucleon (NN) interactions, also involves three-nucleon forces (3NFs) [1–3]. Using these algorithms and standard, (semi)phenomenological nucleon-nucleon interactions alone or supplemented by three-nucleon force model, numerous investigations of 3N bound states and reactions in the 3N continuum have been carried out. High precision nucleon-nucleon potentials such as the AV18 [4], CD Bonn [5], Nijm I and II [6] NN forces, which provide a very good description of the nucleon-nucleon data up to about 350 MeV, have been used. They have also been combined with model 3N forces such as the 2π-exchange Tucson-Melbourne (TM99) 3NF [7] or the Urbana IX model [8].

When realistic NN forces are used to predict binding energies of three-nucleon systems they typically underestimate the experimental bindings of ^{3}H and ^{3}He by about 0.5-1 MeV [9, 10]. This missing binding energy can be corrected for by introducing a three-nucleon force into the nuclear Hamiltonian [9]. Also the study of elastic nucleon-deuteron (Nd) scattering and nucleon induced deuteron breakup revealed a number of cases where the nonrelativistic description using only pairwise forces is insufficient to explain the data. The best studied case at low energies is the vector analyzing power in elastic Nd scattering for which a large discrepancy exists in the region of its maximum around c.m. angles $\theta_{c.m.} \sim 125^o$ and for incoming nucleon energies below ~ 20 MeV [2, 11, 12]. For the elastic scattering angular distribution at such energies, negligible effects of 3NF's have been found and theory based on realistic NN forces agrees well with the data [2, 11].

That picture changes with increasing energy of the Nd system. Generally, the studied discrepancies between experiment and theory using only NN potentials become larger and adding a three-nucleon force to the pairwise interactions leads in some cases to a better description of the data. The elastic Nd angular distribution in the region of its minimum and at backward angles is the best known example [13, 14]. The clear discrepancy in these angular regions at energies up to $E_{\mathrm{lab,\,N}} \sim 100$ MeV between a theory using only NN potentials and the cross section data can be removed by adding standard models of three-nucleon forces to the nuclear Hamiltonian. Such 3NFs are adjusted for a given NN potential to reproduce the experimentally observed binding energy of ^{3}H and ^{3}He [11, 13, 14]. At energies higher than ~ 100 MeV current 3NFs only partially improve

the description of cross section data and the remaining discrepancies, which increase with energy, indicate the possibility of relativistic effects. The need for a relativistic description of three-nucleon scattering was realized when precise measurements of the total cross section for neutron-deuteron (nd) scattering [15] were analyzed within the framework of nonrelativistic Faddeev calculations [16]. NN forces alone were insufficient to describe the data above $\sim$ 100 MeV. The effects due to the relativistic kinematics considered in [16] at higher energies were comparable in magnitude to the effects due to 3NFs. These results provided further motivation to study relativistic effects in the three nucleon continuum in a systematic way.

Subsequent studies of relativistic effects in the three-nucleon continuum [17–20] revealed, that when the non-relativistic form of the kinetic energy is replaced by the relativistic form and a proper treatment of the relativistic dynamics is introduced, the elastic scattering cross section is only slightly increased at backward angles and higher energies while spin observables are practically unchanged. These results led to the conclusion that discrepancies between data and theory at higher energies must reflect the action of 3NF's which have to be included in the nuclear Hamiltonian.

The main drawback of all those studies was inconsistency between applied NN interactions and 3NFs. With the advent of effective field theoretical methods in the form of chiral perturbation theory, it became possible to construct consistent two- and many-nucleon forces. In this way an exciting possibility to study few-nucleon systems and their reactions with consistent two- and many-nucleon interactions has emerged.

In [21], the above mentioned inconsistency was removed and low-energy 3N continuum were investigated with chiral next-to-next-to-leading order (N^2LO) NN and 3N forces. The NN interaction in that order, however, does not describe the NN experimental phase-shifts in a sufficiently wide energy range to allow application of those forces at higher energies.

In [22–24] and [25, 26], precise two-nucleon potentials have been developed at next-to-next-to-next-to-leading order (N^3LO) of the chiral expansion. They reproduce experimental NN phase-shifts [27, 28] in a wide energy range and practically with the same high precision as realistic (semi)phenomenological NN potentials. The necessary work to derive the consistent chiral 3NF's at N^3LO has been accomplished in [29, 30] and [31]. At that order, six different topologies contribute to the 3NF. Three of them are of a long- and intermediate-range [29] and are given by two-pion (2π) exchange, two-pion-one-pion (2π-1π) exchange and the so-called ring diagrams. They are supplemented by the shorter-range 1π-contact and three-nucleon-contact components, which appear first at N^2LO, by the two-pion-exchange-contact (2π-contact) term as well as by the leading relativistic corrections to the three-nucleon force [30].

The results of Refs. [22, 23, 25, 29, 30] enable one to perform, for the first time, consistent calculations of three-nucleon reactions at N^{3}LO order of chiral expansion. The 3NF at this order does not involve any new unknown low-energy constants (LECs) and depends only on two free parameters, c_D and c_E, which parametrize the strengths of the leading 1π-contact and the three-nucleon-contact terms. Their values need to be fixed (at given order) from a fit to a few-nucleon data. Among the few possible observables that have been used in this connection one can mention the triton binding energy, the nd doublet scattering length $^2a_{nd}$ [21], the ^{4}He binding energy [32, 33] along with the point proton rms radius [34], the properties of light nuclei, or the triton β decay rate [35]. Notice that the first three observables are known to be strongly correlated and therefore might not be the best choice for the determination of c_D and c_E.

Application of N^{3}LO 3NF in few-body calculations is challenging due to its very rich and complicated operator structure. The large number of terms in the 3NF at N^{3}LO [29, 30] requires an efficient method of performing partial-wave decomposition. Recently such a method, which runs under the name of automatized partial-wave decomposition (aPWD), was proposed in [36–38]. In that approach, the matrix elements in the 3N momentum-space partial wave basis for different terms contributing to N^{3}LO 3NF are obtained in two consecutive steps. First, the spin-momentum and isospin parts of three-nucleon interactions are computed using symbolic algebra systems. The resulting momentum-dependent functions are then integrated numerically in five dimensions over angular variables. The major advantage of this method is its generality since it can be applied to any momentum-spin-isospin operator. Application of that method for higher angular momenta requires large computer resources. Therefore, in this first study of the 3N continuum with full N^{3}LO chiral force, we restrict ourselves to low energies only. In that region of incoming neutron laboratory (lab.) energies below ~ 30 MeV, the most challenging observables are the nd elastic scattering analyzing power and cross sections in symmetric space star and neutron-neutron quasi-free-scattering configurations of the nd breakup reaction. The discrepancies between data and theory for these observables could not be removed with standard NN and 3NFs [39].

Our paper is organized as follows. In Sec. II we describe our method to determine the nuclear Hamiltonian by fixing the two parameters c_D and c_E in the chiral N^{3}LO 3NF. This is achieved by first requiring reproduction of the ^{3}H binding energy which leads to pairs of allowed (c_D, c_E) values. Using the experimental data for an additional 3N observable, which in our case is taken to be the doublet nd scattering length $^2a_{nd}$, fixes completely the nuclear Hamiltonian at N^{3}LO. Based on the resulting Hamiltonian, we discuss in Sec. III some results for low-energy elastic nd scattering observables while in Sec. IV the results for selected low-energy nd breakup configurations

are presented. We summarize and conclude in Sec. V.

II. DETERMINATION OF NUCLEAR HAMILTONIAN AT N^{3}LO

Neutron-deuteron scattering with neutrons and proton interacting through a NN interaction v_{NN} and a 3NF $V_{123} = V^{(1)}(1+P)$, is described in terms of a breakup operator T satisfying the Faddeev-type integral equation [1–3]

$$T|\phi\rangle \;=\; tP|\phi\rangle + (1+tG_0)V^{(1)}(1+P)|\phi\rangle + tPG_0T|\phi\rangle + (1+tG_0)V^{(1)}(1+P)G_0T|\phi\rangle. \quad (1)$$

The two-nucleon t-matrix t is the solution of the Lippmann-Schwinger equation with the interaction v_{NN}. $V^{(1)}$ is the part of a 3NF which is symmetric under the interchange of nucleons 2 and 3. The permutation operator $P = P_{12}P_{23} + P_{13}P_{23}$ is given in terms of the transposition operators, P_{ij}, which interchange nucleons i and j. The incoming state $|\phi\rangle = |\mathbf{q}_0\rangle|\phi_d\rangle$ describes the free nd motion with relative momentum $\mathbf{q}_0$ and the deuteron state $|\phi_d\rangle$. Finally, G_0 is the resolvent of the three-body center of mass kinetic energy. The amplitude for elastic scattering leading to the corresponding two-body final state $|\phi'\rangle$ is then given by [2, 3]

$$\langle\phi'|U|\phi\rangle \;=\; \langle\phi'|PG_0^{-1}|\phi\rangle + \langle\phi'|PT|\phi\rangle + \langle\phi'|V^{(1)}(1+P)|\phi\rangle + \langle\phi'|V^{(1)}(1+P)G_0T|\phi\rangle, \quad (2)$$

while for the breakup reaction one has

$$\langle\phi_0'|U_0|\phi\rangle \;=\; \langle\phi_0'|(1+P)T|\phi\rangle, \quad (3)$$

where $|\phi_0'\rangle$ is the free three-body breakup channel state.

The nuclear Hamiltonian at N^{3}LO of the chiral expansion is fixed by specifying the values of LECs c_D and c_E which parametrize the strengths of the leading 1π-contact and the three-nucleon-contact terms. To determine them we follow the approach of Ref. [21] and use the experimental triton binding energy $E(^3H)$ and the nd doublet scattering length $^2a_{nd}$ as two observables from which c_D and c_E can be obtained. The procedure can be divided into two steps. First, the dependence of $E(^3H)$ on c_E for a given value of c_D is determined. The requirement to reproduce the experimental value of the triton binding energy yields a set of pairs c_D and c_E. This set is then used in the calculations of $^2a_{nd}$, which allows us to find the values of c_D and c_E describing both observables simultaneously. As already emphasized above, using the triton binding energy and the nd doublet scattering length is probably not the optimal way to fix the parameters in the 3NF due the strong correlation between these two observables. We will discuss this issue in the next two sections and present results obtained by relaxing the condition to reproduce $^2a_{nd}$.

We compute the ^{3}H wave function using the method described in [9], where the full triton wave function $|\Psi\rangle = (1+P)|\psi\rangle$ is given in terms of its Faddeev component ψ, which fulfills the Faddeev equation

$$|\psi\rangle = G_0 t P|\psi\rangle + (1+G_0 t)G_0 V^{(1)}(1+P)|\psi\rangle. \tag{4}$$

The doublet scattering length $^2a_{nd}$ is calculated using (c_D,c_E) pairs, which reproduce the correct value of $E(^3H)$. To this end, we solve the Faddeev equation (1) for the auxiliary state $T|\phi\rangle$ at zero incoming energy [40]. We refer to [2, 3, 41] for a general overview of 3N scattering and for more details on the practical implementation of the Faddeev equations.

In this first study, where the full N^{3}LO 3NF is applied, we restrict ourselves to nd reactions at low energies, $E_{\mathrm{lab,\,n}} < 20$ MeV. At such low energies it is sufficient to include NN force components with a total two-nucleon angular momenta $j \leq 3$ in 3N partial-wave states with the total 3N system angular momentum below $J \leq 25/2$. For the 3NF it is sufficient to incorporate its matrix elements with $j \leq 3$ and $J \leq 5/2$.

Here and in what follows, we employ the N^{3}LO chiral NN potential of Ref. [22, 23]. From among five versions corresponding to different sets of cut-off parameters used to regularize the Lippmann-Schwinger equation and in spectral function regularization, namely (450, 500) MeV, (450, 700) MeV, (550, 600) MeV, (600, 500) MeV, and (600, 700) MeV, we applied for the present study two N^{3}LO chiral NN potentials with cut-off sets (450, 500) MeV and (450, 700) MeV, denoted in the following by 201 and 204, respectively. Only for these two sets of cut-offs were we able to determine the LECs c_D and c_E using our procedure.

In Figs. 1a and 1b, the sets of (c_D, c_E) values which reproduce the experimental binding energy of ^{3}H are shown, while in Figs. 1c and 1d the resulting values of the doublet nd scattering length $^2a_{nd}$ obtained with such combinations of (c_D, c_E) are visualized. In the case of the 201 N^{3}LO NN chiral potential a wide range of c_D values have been checked and the existence of a pole in the scattering length for $c_D \approx -8$ found (see Fig. 1c). That pole-like behavior reflects the emergence of an excited state for that particular 3N Hamiltonian. The requirement to reproduce, in addition to the binding energy of ^{3}H, also the nd doublet scattering length leads to the values $(c_D = 13.78, c_E = 0.372)$ for 201 and to $(c_D = 9.095, c_E = -0.0845)$ for 204 chiral N^{3}LO NN potential. In the following section we discuss the ambiguities of such a determination of (c_D, c_E). The resulting c_D values are unnaturally large. The corresponding N^{2}LO values are natural and amount to $(c_D = -0.14, c_E = -0.319)$ and $(c_D = 2.43, c_E = 0.113)$ for (450, 500) MeV and (450, 700) MeV cut-off sets, respectively. It seems that such unnaturally large values of c_D are not

restricted only to the two cut-off sets used in the present study. Namely in [42] an application of N^{3}LO 3NF, however with relativistic $1/m$ corrections and short-range 2π-contact term omitted, also led to unnaturally large c_D values for all five cut-off combinations. We hope that new generations of chiral forces with other regularization schemes will cure this problem [43]. We also plan to use other 3N observables, for example triton β-decay rate instead of $^2a_{nd}$, to fix values of LECs c_D and c_E.

III. LOW-ENERGY ELASTIC ND SCATTERING

At low energies of the incoming neutron, the most interesting observable is the analyzing power A_y for nd elastic scattering with polarized neutrons. Theoretical predictions of standard high-precision NN potentials fail to explain the experimental data for A_y. The data are underestimated by $\sim 30\%$ in the region of the A_y maximum which occurs at c.m. angles $\Theta_{c.m.} \sim 125^o$. Combining standard NN potentials with commonly used models of a 3NF, such as e.g. the TM99 or Urbana IX models, removes approximately only half of the discrepancy with respect to the data (see Fig. 2).

When instead of standard forces chiral NN interactions are used, the predictions for A_y vary with the order of chiral expansion [22, 23]. In particular, as reported in Ref. [21], the NLO results overestimate the A_y data while N^{2}LO NN forces seem to provide quite a good description of them (see Fig. 2). Only when N^{3}LO NN chiral forces are used, a clear discrepancy between theory and data emerge in the region of A_y maximum, which is similar to the one for standard forces. This is visualized in Fig. 2, where bands of predictions for five versions of the Bochum NLO, N^{2}LO and N^{3}LO potentials with different cut-off parameters used for the Lippmann-Schwinger equation and the spectral function regularizations are shown [23]). Such behaviour of A_y predictions at different orders in the chiral expansion can be traced back to a high sensitivity of A_y to ^3P_j NN force components and to the fact, that only at N^{3}LO of chiral expansion the experimental ^3P_j phases [27, 28], especially the $^3P_2$-$^3F_2$ ones, are properly reproduced [42].

It is interesting to study whether the consistent chiral N^{3}LO 3NF's can explain the low-energy A_y-puzzle. In the present investigation, we, for the first time include *all* contributions to N^{3}LO 3NF: long-range contributions comprising 2π-exchange, $2\pi - 1\pi$-exchange, ring components and relativistic 1/m corrections together with short range 1π-contact, three-nucleon-contact and 2π-contact terms. In Fig. 3 we show by dashed-dotted (blue) line the results for A_y based on the values of the c_E and c_D parameters which reproduce the triton binding energy and $^2a_{nd}$ scattering length. It turns out that adding the full N^{3}LO 3NF does not improve the description of A_y. On

the contrary, adding the chiral N^{3}LO 3NF lowers the maximum of A_y with respect to the chiral N^{3}LO NN prediction, shown by the solid (red) line, thus, increasing the discrepancy between the theory and the data.

In order to check the restrictiveness of the requirement to reproduce, in addition to the ^{3}H binding energy, also the experimental value of $^2a_{nd}$, we show in Fig. 3 also a band of predictions for (c_E, c_D) pairs from Fig. 1a and 1b. Even after relaxing the requirement to reproduce $^2a_{nd}$, the A_y-puzzle cannot be explained by the N^{3}LO NN and 3NF.

It is interesting to see how different components of the N^{3}LO 3NF contribute to A_y. Taking in addition to the NN N^{3}LO chiral force only the 2π-exchange term with leading 1π-contact and three-nucleon-contact terms (these three topologies appear for the first time at N^{2}LO) lowers the maximum of A_y (see Fig. 4, solid (cyan) line). When, in addition, the short-range 2π-contact component is included, the value of A_y practically remains unchanged (dashed-dotted (magenta) line in Fig. 4). This shows that contributions of the 2π-contact term are negligible at those energies. The long-range $2\pi - 1\pi$-exchange and ring terms lower significantly the maximum of A_y (in Fig. 4 dotted (maroon) and dashed (green) lines, respectively). Finally, inclusion of the relativistic $1/m$ contribution leaves the maximum of A_y practically unchanged (dashed-double-dotted (blue) line in Fig. 4). It should be pointed out that when taking into account the $1/m$ corrections to the N^{3}LO 3NF, one should also include the corresponding relativistic corrections in the NN force and, in addition, also relativistic corrections to the kinetic energy, which are formally of the same importance. This would considerably complicate the calculation. In our present work, we do not take into account such corrections and employ the standard nonrelativistic framework. This seems to be justified in view of the low energies considered in this paper and the very small effects caused by relativistic $1/m$ corrections to the 3NFs found in this study. Last but not least, we emphasize that the contributions of the individual 3NF topologies to the A_y puzzle are not observable and depend, in particular, on the regularization scheme and employed NN forces.

It is important to address the question of uniqueness of our approach to determine the constants c_D and c_E. To this aim, we checked how taking instead of $^2a_{nd}$ a different nd observable would influence determination of c_D and c_E. The low-energy elastic nd scattering cross section is an observable which seems to be reasonably well described by standard theory [47]. In Fig. 5 we show (orange) bands of predictions for the nd elastic scattering cross section at $E_{\mathrm{lab,\,n}} = 6.5$ MeV and 10 MeV obtained with full N^{3}LO chiral force with (c_D, c_E) values from Figs. 1a and 1b which reproduce only the experimental binding energy of ^{3}H. These bands are relatively narrow for version 204 and angles $\Theta_{c.m.} > 130^\circ$ and start to become broader at smaller angles. At forward

angles the requirement that only the binding energy of ^{3}H is reproduced leads to a wide range of predictions for the cross section. The solid (red) lines in Fig. 5 are predictions of the N^{3}LO chiral NN potential and the dotted (maroon) lines show cross sections for the full N^{3}LO chiral force with constants c_D and c_E fixed by requirement that the doublet nd $^2a_{nd}$ scattering length is also reproduced. For comparison to standard potential cross sections in Fig. 5 also the CD Bonn potential results are shown by solid (blue) lines. The backward angle nd elastic scattering cross section data are properly described by standard, high precision NN potentials [47]. To fix values of c_D and c_E it would be desirable to have forward angle cross section data. Assuming that in this angular region the data will be properly described by our theory indicates that replacing $^2a_{nd}$ by cross section would lead to consistent c_D and c_E values in both approaches.

IV. LOW-ENERGY ND BREAKUP

Among numerous kinematically complete configurations of the nd breakup reaction the SST and QFS configurations have attracted special attention. The cross sections for these geometries are very stable with respect to the underlying dynamics. Different potentials, alone or combined with standard 3NFs, lead to very similar results for the cross sections [39] which deviate significantly from available SST and neutron-neutron (nn) QFS data. At low energies, the cross sections in the SST and QFS configurations are dominated by the S-waves. For the SST configuration, the largest contribution to the cross section comes from the $^3S_1$ partial wave, while for the nn QFS the $^1S_0$ partial wave dominates. Neglecting rescattering, the QFS configuration resembles free NN scattering. For free, low-energy neutron-proton (np) scattering one expects contributions from $^1S_0$ np and $^3S_1$ force components. For free nn scattering, only the $^1S_0$ nn channel is allowed. This suggests that the nn QFS is a powerful tool to study the nn interaction. The measurement of np QFS cross sections have revealed good agreement between the data and theory [52], thus confirming the knowledge of the np force. For the nn QFS it was found that the theory underestimates the data by $\sim 20\%$ [52]. The large stability of the QFS cross sections with respect to the underlying dynamics means that, assuming correctness of the nn QFS data, the present day $^1S_0$ nn interaction is probably incorrect [39, 53, 54].

Also the chiral N^{3}LO forces with all components of the 3NF included are not an exception and cannot explain the discrepancy between the theory and data found for the SST configuration [48] (Fig. 6). The solid (black) line shows the cross section when only NN chiral N^{3}LO force is active. Adding the full N^{3}LO 3NF with c_D and c_E pairs reproducing the experimental binding energy of

^{3}H and nd doublet scattering length leads to dashed-double-dotted (blue) line. At 13 MeV, it lies only slightly below the NN potential prediction indicating only small 3NF effects at this energy.

It is interesting to see how the SST cross section depends on the choice of parameters (c_D,c_E) which enter the N^{3}LO nuclear Hamiltonian. In Fig. 6, the SST cross sections at $E_{\rm lab,\,n} = 13$ MeV are shown for a number of c_D and c_E pairs which reproduce only the experimental binding energy of ^{3}H (taken from Fig. 1a and 1b). For the 201 N^{3}LO nuclear Hamiltonian (see Fig. 6a) decreasing the value of c_D leads to big changes of the SST cross section. Starting from $c_D = 13.78$, which reproduce also $^2a_{nd}$, and decreasing it to $c_D = 9$ leads to only small changes of the SST cross sections. Further lowering of c_D down to $c_D = -3$ reduces the cross section and the discrepancy to nd data at 13 MeV is drastically increased. If we continue to reduce the c_D value the SST cross section rises, however, it remains always below the pure NN prediction. For the 204 N^{3}LO nuclear Hamiltonian the changes of the SST cross section are not so drastic and decrease of the c_D reduces the cross section (see Fig. 6b). Thus, in spite of the strong sensitivity of the SST cross sections to values of c_D and c_E, it is not possible to describe the available experimental data for the SST nd cross sections at 13 MeV even allowing for pairs of (c_D,c_E) which do not reproduce $^2a_{nd}$.

As shown in Fig. 7 the behaviour of the QFS cross section is different from SST. This configuration also appears to be sensitive to changes of c_D and c_E values. Here, decreasing c_D for the 201 N^{3}LO nuclear Hamiltonian leads first to the increase of the QFS cross section up to $c_D \sim -1.0$. Further lowering the value of c_D reduces the QFS cross section (see Fig. 7a). For the 204 N^{3}LO nuclear Hamiltonian decreasing c_D leads to the increase of the QFS cross section (see Fig. 7b). The values of c_D and c_E which reproduce the ^{3}H binding energy and $^2a_{nd}$ lead only to a slight increase of the QFS cross section with respect to the N^{3}LO NN prediction and thus to small 3NF effects.

V. SUMMARY AND OUTLOOK

Recent efforts towards the derivation and implementation of the N^{3}LO 3NF allowed us, for the first time, to apply the full chiral N^{3}LO Hamiltonian to the low-energy nd elastic scattering and breakup reactions. The nuclear Hamiltonian at that order of the chiral expansion is unambiguously given after fixing the two constants c_D and c_E which determine the strengths of the 1π-contact and three-nucleon-contact components of the N^{3}LO chiral 3NF. We determined these low-energy constants by requiring reproduction of the binding energy of ^{3}H and the doublet nd scattering length $^2a_{nd}$. We found indications that using low-energy nd elastic scattering cross section instead of $^2a_{nd}$ would probably lead to similar values of these parameters.

It turns out that applying the full N^{3}LO 3NF with specific cut-off parameters used in this study cannot explain the low-energy A_y-puzzle. Contrary to the 3NF effects found for A_y with standard NN potentials combined with 3NF models such as TM99 or Urbana IX, where the inclusion of the 3NF decreased the discrepancy to data by about $\sim$ 50%, the chiral N^{3}LO 3NF combined with the NN potential of Ref. [22] lowers the maximum of A_y increasing the discrepancy. It should, however, be emphasized that the low-energy 3N A_y is a fine-tuned observable which is very sensitive to changes in ^3P_j NN force components as well as to P-waves in the Nd system [55, 56]. Thus, the disagreement with the data must be interpreted with considerable caution. Our result suggests the lack of some spin-isospin-momenta structures in the N^{3}LO 3NF. However, possible inaccuracies in low-energy ^3P_j NN phase-shifts cannot be excluded. The 3NF derived in the standard formulation of chiral perturbation theory based on pions and nucleons as the only explicit degrees of freedom is known to miss certain significant intermediate-range contributions of the $\Delta(1232)$ resonance at N^{3}LO, which, to some extent, are accounted for only at N^{4}LO and higher orders [57, 58]. It would therefore be interesting, to apply the recently derived N^{4}LO 3NF [57, 58] in calculations of nd reactions together with subleading contributions to the three-nucleon contact interactions [59]. The short-range 3N forces at N^{4}LO which contribute to Nd P-waves may solve the A_y-puzzle in a trivial way.

We found that cross sections in kinematically complete SST and QFS nd breakup configurations at low energies are quite sensitive to the values of c_D and c_E. For their values fixed by the experimental binding energy of ^{3}H and $^2a_{nd}$ only small 3NF effects were found in these configurations. Large discrepancies with the data remain in these configurations.

For the SST geometry at 13 MeV, there is a serious discrepancy between theory and two independent nd data sets of Refs. [48, 50] as well as between theory and proton-deuteron (pd) data of Ref. [51]. While the nd data lie $\sim$ 20% above the theory, the pd data lie $\sim$ 10% below theory and $\sim$ 30% below nd data. Recent pd calculations with Coulomb force included show practically negligible effects of the proton-proton Coulomb force for this configuration [60]. The observed large splitting between the nd and pd data indicates either that there are large isospin-breaking effects or that the data are not consistent.

Higher-energy nd reactions, in which clear evidence of large 3NF effects was found, call for applications of the full N^{3}LO force. Studies of the cut-off dependence of N^{3}LO NN chiral interaction in higher-energy nd elastic scattering revealed preference for larger cut-off values [42]. The use of lower cut-offs would preclude applications of N^{3}LO chiral dynamics in that interesting region of energies. It is important to address the issue of reducing finite-cutoff artifacts and increasing the

accuracy of chiral nuclear forces prior to applying the chiral N^{3}LO Hamiltonian at higher energies. In addition, one needs to explore different possibilities to determine the LECs entering the 3NF in view of the known strong correlations between e.g. the ^{3}H and ^{4}He binding energies and the nd doublet scattering lengths, see [61] for a related discussion. Last but not least, more effort should be invested into providing a reliable estimation of the theoretical uncertainty at a given order in the chiral expansion. Work along these lines is in progress.

Acknowledgments

This study has been performed within Low Energy Nuclear Physics International Collaboration (LENPIC) project and was supported by the Polish National Science Center under Grant No.DEC-2013/10/M/ST2/00420. It was also supported in part by the European Community-Research Infrastructure Integrating Activity "Exciting Physics Of Strong Interactions" (acronym WP4 EPOS) under the Seventh Framework Programme of EU, the ERC project 259218 NUCLEAREFT, by the Foundation for Polish Science MPD program, cofinanced by the European Union within the Regional Development Fund, by the US Department of Energy under Grant Nos. DESC0008485 (SciDAC/NUCLEI) and DE-FG02-87ER40371, by the US National Science Foundation under Grant No. PHYS-0904782, and by the ERC Grant No. 307986 STRONGINT. The numerical calculations have been performed on the supercomputer clusters of the JSC, Julich, Germany, the Ohio Supercomputer Centre, USA (Project PAS0680) and the Argonne Leadership Computing Facility (ALCF) at Argonne National Laboratory (Resource Project: NucStructReact), where an award of computer time was provided by the Innovative and Novel Computational Impact on Theory and Experiment (INCITE) program. This research used resources of the ALCF, which is supported by the Office of Science of the U.S. Department of Energy under contract DE-AC02-06CH11357.

[1] H. Witała, T. Cornelius and W. Glöckle, Few-Body Syst. **3**, 123 (1988).

[2] W. Glöckle, H. Witała, D. Hüber, H. Kamada, J. Golak, Phys. Rep. **274**, 107 (1996).

[3] D. Hüber, H. Kamada, H. Witała, and W. Glöckle, Acta Physica Polonica **B28**, 1677 (1997).

[4] R.B. Wiringa, V.G.J. Stoks, R. Schiavilla, Phys. Rev. C**51**, 38 (1995).

[5] R. Machleidt, F. Sammarruca, and Y. Song, Phys. Rev. C**53**, R1483 (1996).

[6] V.G.J. Stoks, R.A.M. Klomp, C.P.F. Terheggen, J.J. de Swart, Phys. Rev. C**49**, 2950 (1994).

[7] S.A. Coon and H.K. Han, Few-Body Syst. **30**, 131 (2001).

[8] B.S. Pudliner et al., Phys. Rev. C**56**, 1720 (1997).

[9] A. Nogga, D. Hüber, H. Kamada, and W. Glöckle, Phys. Lett. B**409**, 19 (1997).

[10] J.L. Friar, G.L. Payne, V.G.J. Stoks, J.J. de Swart, Phys. Lett. B**311**, 4 (1993).

[11] H. Witała et al., Phys. Rev. C**63**, 024007 (2001).

[12] A. Kievsky, M. Viviani, and S. Rosati, Phys. Rev. C**64**, 024002 (2001).

[13] H. Witała, W. Glöckle, D. Hüber, J. Golak, and H. Kamada, Phys. Rev. Lett. **81**, 1183 (1998).

[14] K. Sekiguchi et al., Phys. Rev. C**65**, 034003 (2002).

[15] W.P. Abfalterer et al., Phys. Rev. Lett. **81**, 57 (1998).

[16] H. Witała et al., Phys. Rev. C**59**, 3035 (1999).

[17] H. Witała, J. Golak, W. Glöckle, H. Kamada, Phys. Rev. **C71**, 054001 (2005).

[18] H. Witała, J. Golak, R. Skibiński, W. Glöckle, W.N. Polyzou, H. Kamada, Phys. Rev. **C77**, 034004 (2008).

[19] H. Witała, J. Golak, R. Skibiński, W. Glöckle, H. Kamada, and W.N. Polyzou, Phys. Rev. **C83**, 044001 (2011).

[20] H. Witała, J. Golak, R. Skibiński, W. Glöckle, H. Kamada, and W.N. Polyzou, Phys. Rev. **C88**, 069904(E) (2013).

[21] E. Epelbaum et al., Phys. Rev. C **66**, 064001 (2002).

[22] E. Epelbaum, W. Glöckle, and U.-G. Meißner, Nucl. Phys. **A747**, 362 (2005).

[23] E. Epelbaum, Prog. Part. Nucl. Phys. **57**, 654 (2006).

[24] E. Epelbaum, H.-W. Hammer and U.-G. Meißner, Rev. Mod. Phys. **81**, 1773 (2009).

[25] D.R. Entem and R. Machleidt, Phys. Rev. C**68**, 041001(R) (2003).

[26] R. Machleidt, D.R. Entem , Phys. Rep. **503**, 1 (2011).

[27] J. R. Bergervoet et al., Phys. Rev. C**41**, 1435 (1990).

[28] V.G.J. Stoks, R.A.M. Klomp, M.C.M. Rentmeester, and J.J. de Swart, Phys. Rev. C**48**, 792 (1993).

[29] V. Bernard, E. Epelbaum, H. Krebs, and U.-G. Meißner, Phys. Rev. C **77**, 064004 (2008).

[30] V. Bernard, E. Epelbaum, H. Krebs, and U.-G. Meißner, Phys. Rev. C**84**, 054001 (2011).

[31] S. Ishikawa and M. R. Robilotta, Phys. Rev. C**76**, 014006 (2007).

[32] A. Kievsky, M. Viviani, L. Girlanda, and L.E. Marcucci, Phys. Rev. C**81**, 044003 (2010).

[33] P. Navràtil, Few-Body Syst. **41**, 117 (2007).

[34] P. Navràtil, V. G. Gueorguiev, J. P. Vary, W. E. Ormand and A. Nogga, Phys. Rev. Lett. **99**, 042501 (2007).

[35] L.E. Marcucci, A. Kievsky, S. Rosati, R. Schiavilla, and M. Viviani, Phys. Rev. Lett. **108**, 052502 (2012).

[36] J. Golak et al., Eur. Phys. J. A**43**, 241 (2010).

[37] R.Skibiński et al., Eur. Phys J. **A47** 48 (2011).

[38] R.Skibiński et al., Phys. Rev. **C84**, 054005 (2011).

[39] H. Witała and W. Glöckle, J. Phys. G: Nucl. Part. Phys. **37**, 064003 (2010).

[40] H. Witała, A. Nogga, H. Kamada, W. Glöckle, J. Golak, R. Skibiński, Phys. Rev. **C68**, 034002 (2003).

[41] W. Glöckle, The Quantum Mechanical Few-Body Problem, Springer-Verlag 1983.

[42] H.Witała, J. Golak, R.Skibiński, and K.Topolnicki, J. Phys. G: Nucl. Part. Phys. **41**, 094011 (2014).

[43] E. Epelbaum, private communication.

[44] W. Tornow et al. Phys. Lett. **B257**, 273 (1991).

[45] W. Tornow, C.R. Howell, R.C. Byrd, R.S. Pedroni, and R.L. Walter, Phys. Rev. Lett. **49**, 312 (1982).

[46] K.Schoen et al., Phys. Rev. **C67**, 044005 (2003).

[47] C.R. Howell et al., Few-Body Syst. **16**, 127 (1994).

[48] H. R. Setze et al., Phys. Lett. **B388**, 229 (1996).

[49] J. Strate et al., J. Phys. G: Nucl. Phys. **14**, L229 (1988).

[50] J. Strate et al., Nucl. Phys. **A501**, 51 (1989).

[51] G. Rauprich et al. Nucl. Phys. **A535**, 313 (1991).

[52] A. Siepe et al., Phys. Rev. **C65**, 034010 (2002).

[53] H. Witała and W. Glöckle, Phys. Rev. **C83**, 034004 (2011).

[54] H. Witała and W. Glöckle, Phys. Rev. **C85**, 064003 (2012).

[55] D. Hüber, J. Golak, H. Witała, W. Glöckle, and H. Kamada, Few-Body Syst. **19**, 175 (1995).

[56] W. Tornow, H. Witała, A. Kievsky, Phys. Rev. **C57**, 555 (1998).

[57] H. Krebs, A. Gasparyan, and E. Epelbaum, Phys. Rev. **C85**, 054006 (2012).

[58] H. Krebs, A. Gasparyan, and E. Epelbaum, Phys. Rev. **C87**, 054007 (2013).

[59] L. Girlanda, A. Kievsky, and M. Viviani, Phys. Rev. C**84**, 014001 (2011).

[60] A. Deltuva, A.C. Fonseca, and P.U. Sauer, Phys. Rev. C**72**, 054004 (2005).

[61] D. Gazit, S. Quaglioni and P. Navratil, Phys. Rev. Lett. **103**, 102502 (2009).

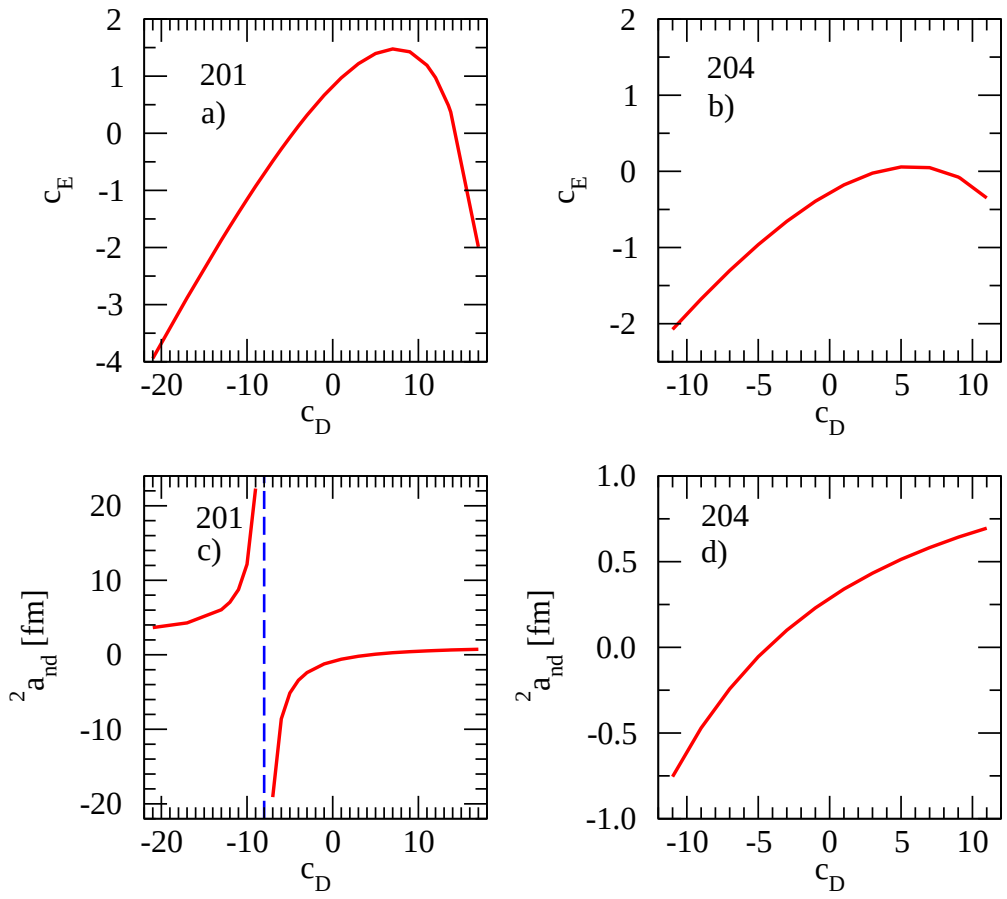

FIG. 1: (color online) The dependence of c_E on c_D for versions 201 (a) and 204 (b) of the N^{3}LO chiral NN Hamiltonian under the condition that the experimental binding energy of ^{3}H is reproduced. In c) and d) the corresponding values for doublet nd scattering length are shown. The experimental value of the doublet nd scattering length is $^2a_{nd} = 0.645(7)$ fm [46].

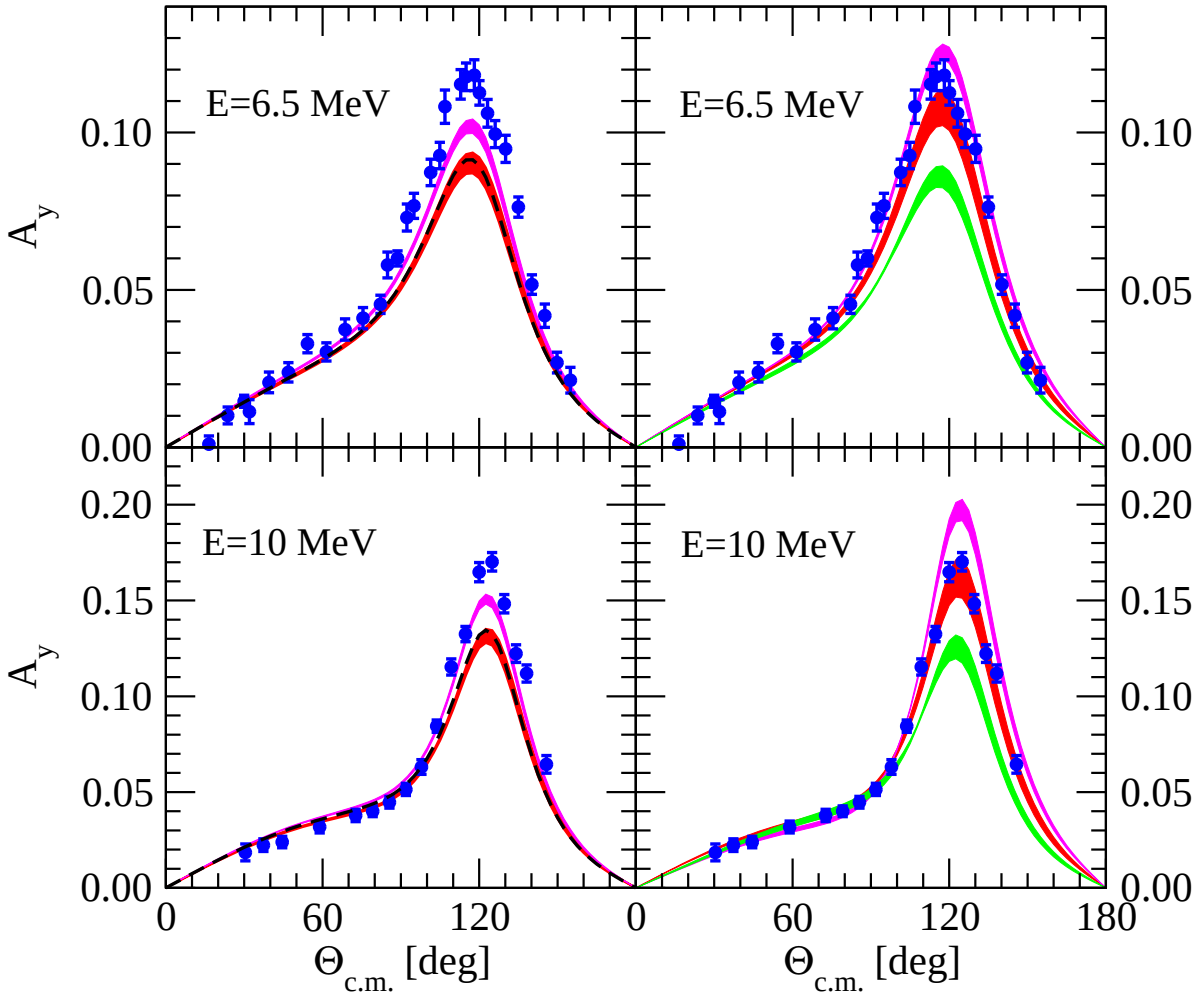

FIG. 2: (color online) The nd elastic scattering analyzing power A_y at $E_{\mathrm{lab,\,n}} = 6.5$ MeV and 10 MeV. In the left panels the bottom (red) band covers predictions of standard NN potentials: AV18, CD Bonn, Nijm1 and Nijm2. The upper (magenta) band results when these potentials are combined with the TM99 3NF. The dashed (black) line shows prediction of the AV18+Urbana IX combination. In the right panels bands of predictions for five versions of chiral NN potentials at different orders of the chiral expansion are shown: NLO - the upper (magenta) band, $\mathrm{N^2LO}$ - the middle (red) band, and $\mathrm{N^3LO}$ - the bottom (green) band. These five versions correspond to different cut-off values used for the Lippmann-Schwinger equation and spectral function regularizations, namely $(450, 500)$ MeV, $(450, 700)$ MeV, $(550, 600)$ MeV, $(600, 500)$ MeV, and $(600, 700)$ MeV [22, 23]. The full circles are nd data from Ref. [44] at 6.5 MeV and from Ref. [45] at 10 MeV.

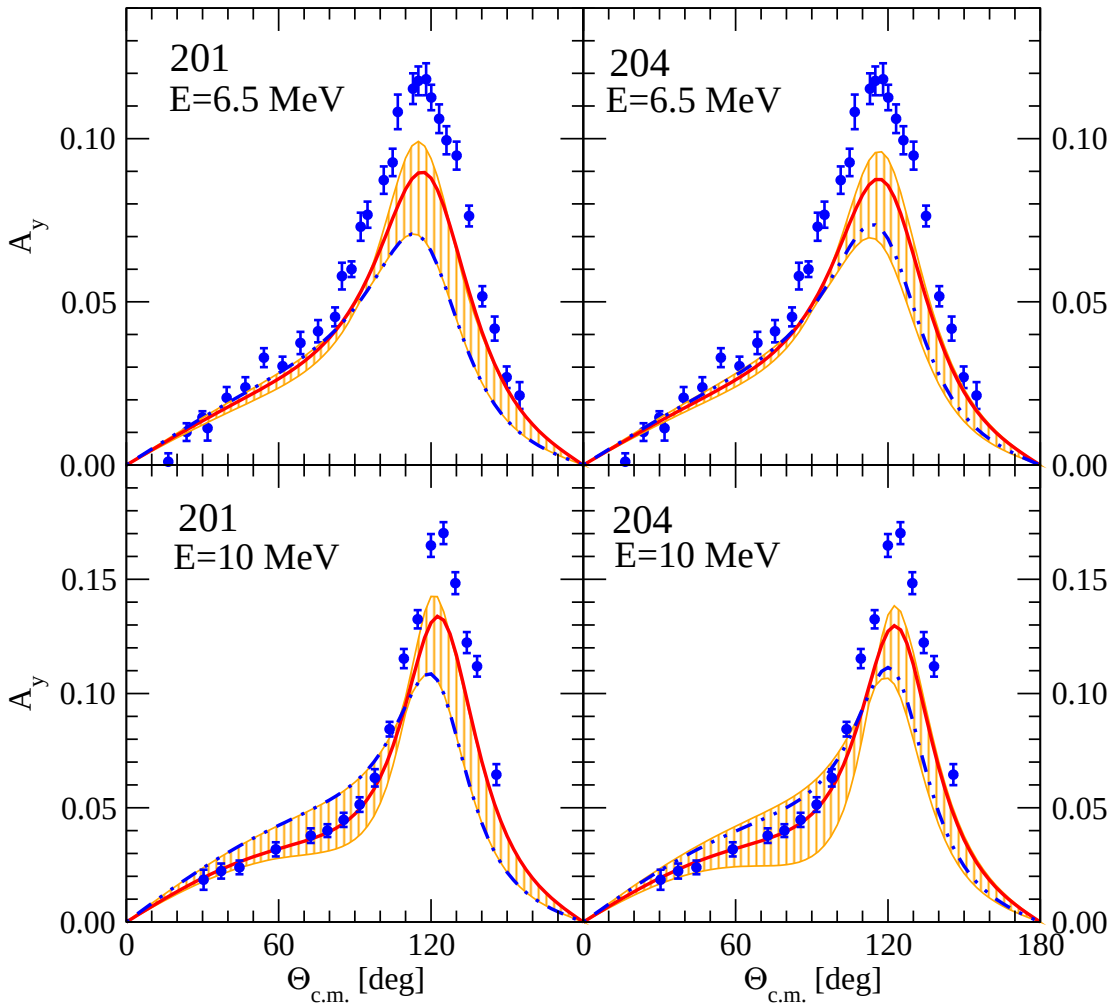

FIG. 3: (color online) The nd elastic scattering analyzing power A_y at $E_{\mathrm{lab,\,n}} = 6.5$ MeV and 10 MeV. The solid (red) lines show predictions of the N^{3}LO chiral NN potential. The dashed-double-dotted (blue) lines result when the chiral NN potential is combined with the full N^{3}LO 3NF with c_D and c_E values reproducing binding energy of ^{3}H and $^2a_{nd}$ scattering length. The (orange) vertically shaded band covers range of predictions for such a combination when pairs of (c_D, c_E) values from Fig. 1a and 1b, which reproduce only triton binding energy, are used. For the description of the data see Fig. 2.

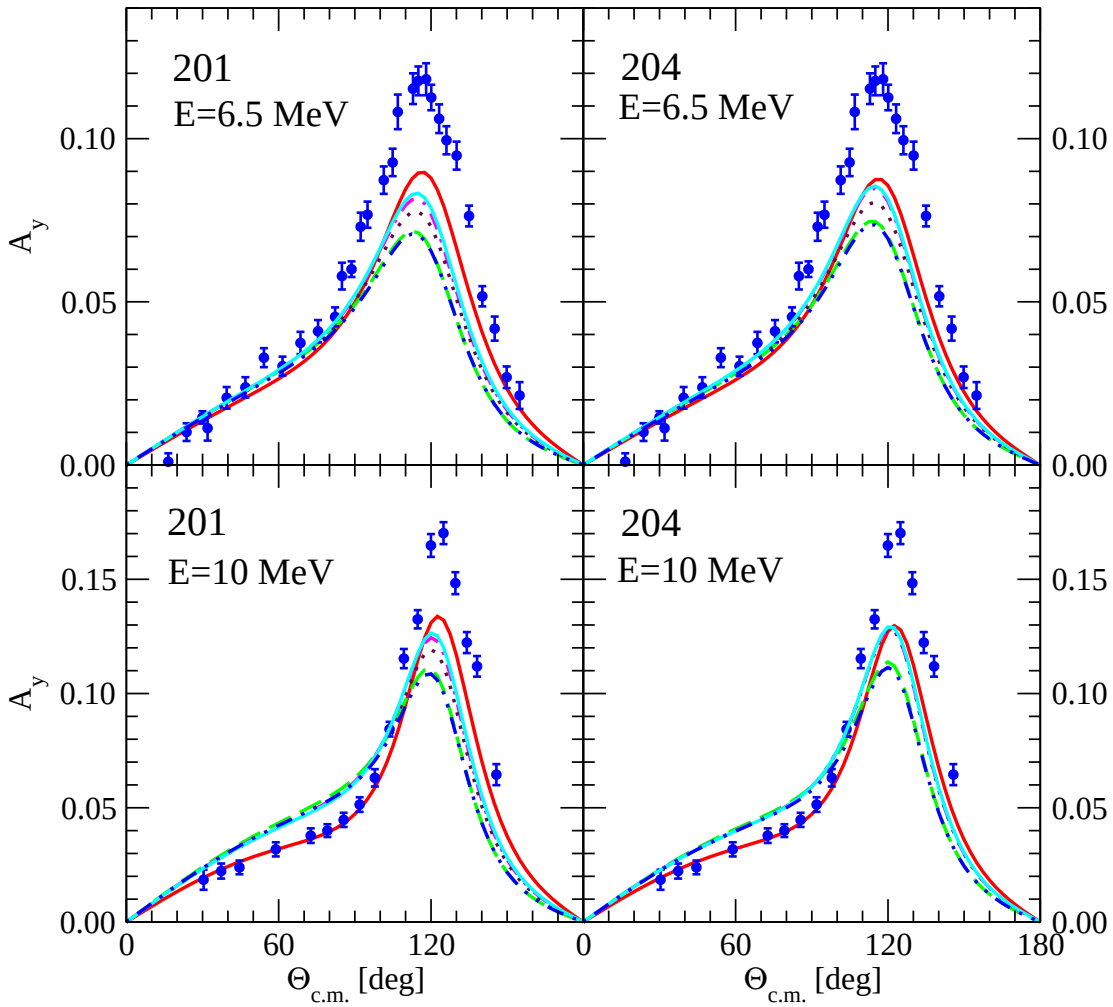

FIG. 4: (color online) The nd elastic scattering analyzing power A_y at $E_{\mathrm{lab,\,n}} = 6.5$ MeV and 10 MeV. The solid (red) line gives the prediction of the N^{3}LO chiral NN potential. Other lines show the importance of different components of the chiral N^{3}LO 3NF when combined with that NN interaction. The solid (cyan), dashed-dotted (magenta), dotted (maroon), and dashed (green) lines result when that NN N^{3}LO force is combined with $\pi\pi + D + E$, $\pi\pi + D + E + 2\pi - \mathit{contact}$, $\pi\pi + 2\pi 1\pi + D + E + 2\pi - \mathit{contact}$, and $\pi\pi + 2\pi 1\pi + \mathit{ring} + D + E + 2\pi - \mathit{contact}$, respectively. The full N^{3}LO result with the relativistic term included is shown by the dashed-double-dotted (blue) line. For the description of the data see Fig. 2.

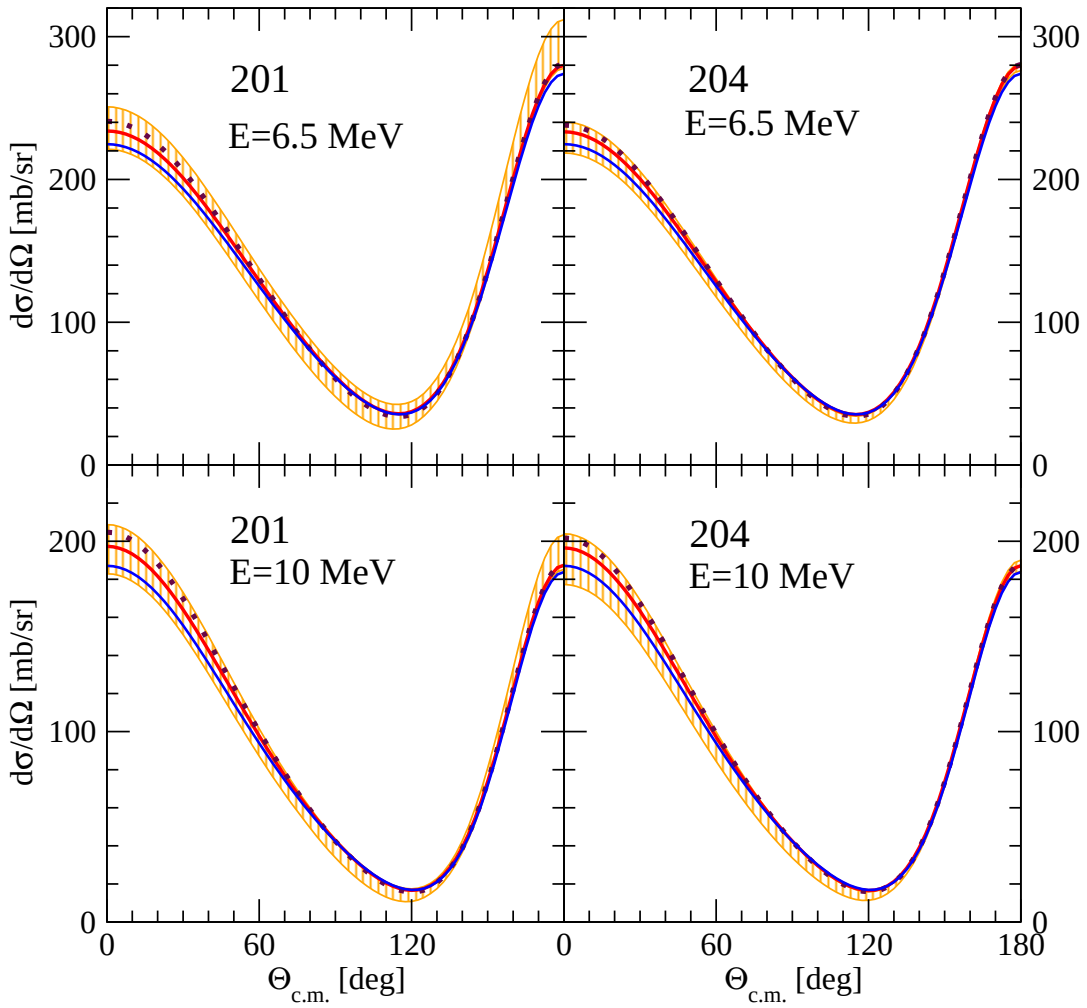

FIG. 5: (color online) The nd elastic scattering angular distributions at $E_{\mathrm{lab,\,n}} = 6.5$ MeV and 10 MeV. The solid (blue) lines show predictions of the CD Bonn potential. The solid (red) lines give predictions of the N^{3}LO chiral NN potential. The dotted (maroon) lines result when the chiral N^{3}LO NN potential is combined with full N^{3}LO 3NF with c_D and c_E values reproducing both binding energy of ^{3}H and $^2a_{nd}$ scattering length. The (orange) vertically shaded band covers the range of predictions for such a combination when pairs of (c_D, c_E) values from Fig. 1a and 1b, which reproduce only triton binding energy, are used.

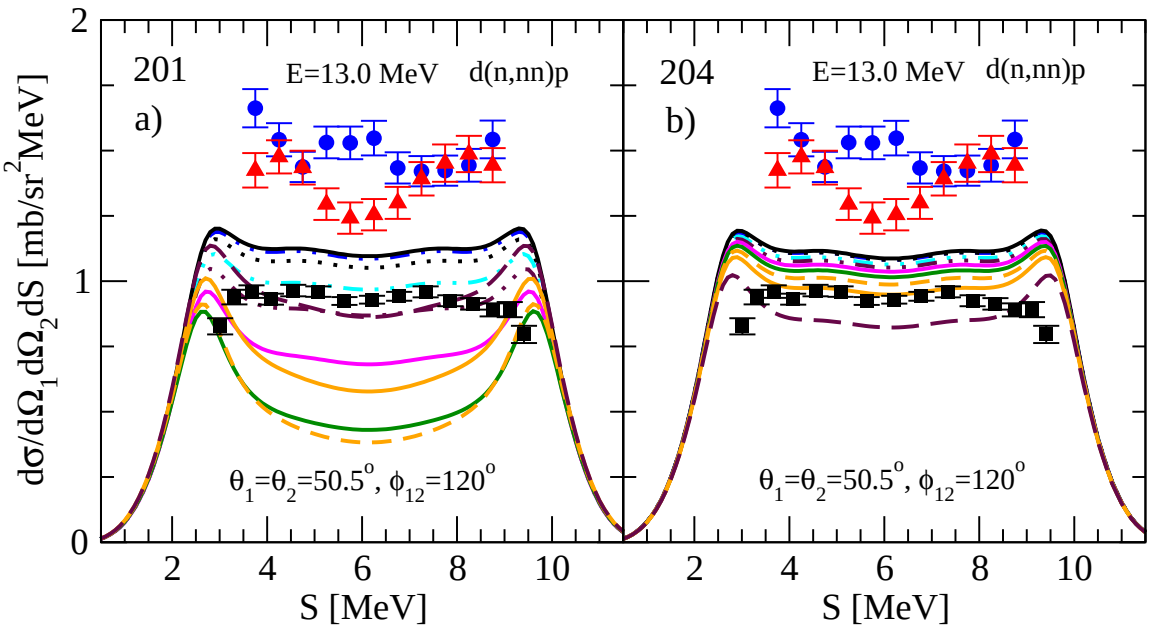

FIG. 6: (color online) The SST nd breakup cross section at incoming neutron lab. energy $E_{\rm lab,\,n} = 13$ MeV as a function of the arc-length S along the kinematical locus in the $E_1 - E_2$ plane. The solid (black) line shows the prediction of the chiral N^{3}LO NN potential alone. The dashed-double-dotted (blue) line results when the full N^{3}LO chiral 3NF with c_D and c_E values reproducing binding energy of ^{3}H and $^2a_{nd}$ is added to the chiral N^{3}LO NN potential. Other lines show the result when that NN force is combined with the full N^{3}LO 3NF with pairs (c_D,c_E) reproducing only the experimental binding energy of ^{3}H from Fig. 1a for a) [Fig. 1b for b)]: (9.0,1.425) [(9.0,-0.0752)] - (black) dotted, (5.0,1.395) [(5.0,0.058)] - (cyan) dashed-double-dotted, (3.0,1.219) [(3.0,-0.023)] - (maroon) dashed-double-dotted), (1.0,0.971) [(1.0,-0.178)] - (magenta) solid, (-1.0,0.6655) [(-1.0,-0.392)] - (green) solid, (-3.0,0.3155) [(-3.0,-0.656)] - (orange) dashed, (-5.0,-0.071) [(-5.0,-0.962)] - (orange) solid, (-9.0,-0.92883) [(-9.0,-1.6759)] - (maroon) dashed. The (blue) circles and (red) triangles are nd data from Ref. [48] and [49, 50], respectively. The (black) squares are proton-deuteron (pd) data of Ref. [51].

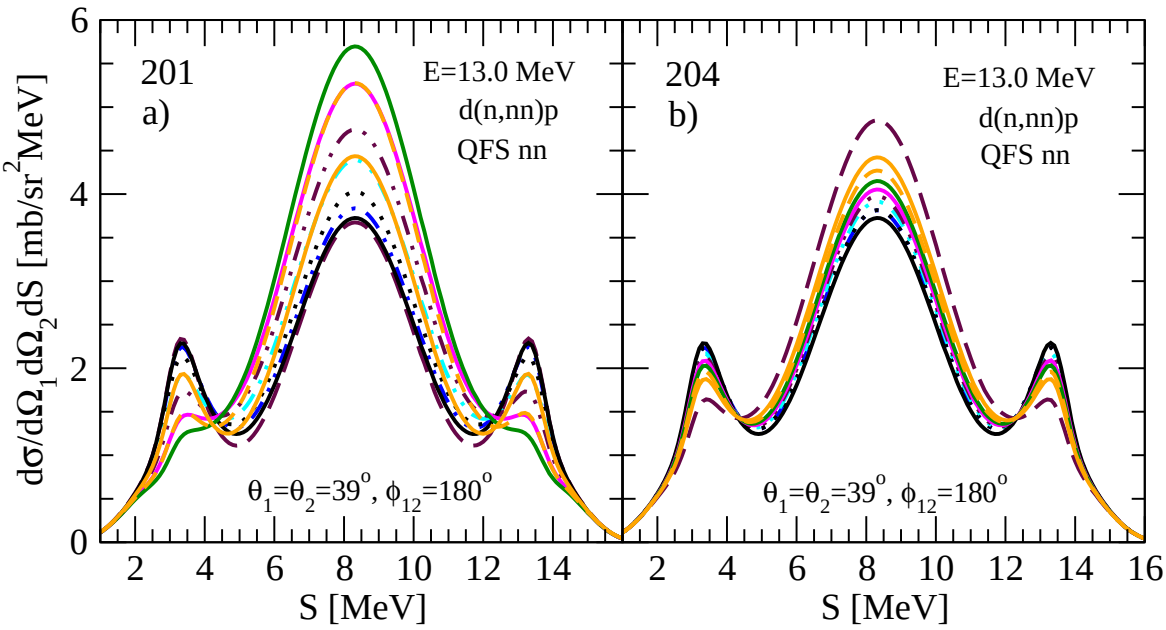

FIG. 7: (color online) The nn QFS nd breakup cross section at incoming neutron lab. energy $E_{\mathrm{lab,\,n}}$ = 13.0 MeV. For an explanation of the lines see Fig. 6.